Journal of Thermal Stresses

ISSN: 0149-5739 (Print) 1521-074X (Online) Journal homepage: https://www.tandfonline.com/loi/uths20

Thermoelasticity and P-wave simulation based on the Cole-Cole model

José M. Carcione, Francesco Mainardi, Stefano Picotti, Li-Yun Fu & Jing Ba

To cite this article: José M. Carcione, Francesco Mainardi, Stefano Picotti, Li-Yun Fu & Jing Ba (2020): Thermoelasticity and P-wave simulation based on the Cole-Cole model, Journal of Thermal Stresses, DOI: 10.1080/01495739.2020.1722772

To link to this article: https://doi.org/10.1080/01495739.2020.1722772

Published online: 19 Feb 2020.

JOURNAL OF THERMAL STRESSES
https://doi.org/10.1080/01495739.2020.1722772

Taylor & Francis
Taylor & Francis Group

Thermoelasticity and P-wave simulation based on the Cole-Cole model

José M. Carcione[a,b], Francesco Mainardi[c], Stefano Picotti[b], Li-Yun Fu[d], and Jing Ba[a]

[a]School of Earth Sciences and Engineering, Hohai University, Nanjing, China; [b]Istituto Nazionale di Oceanografia e di Geofisica Sperimentale (OGS), Trieste, Italy; [c]Department of Physics, University of Bologna, Bologna, Italy; [d]School of Geosciences, China University of Petroleum (East China), Qingdao, China

ABSTRACT

The classical Zener model of thermoelasticity can be represented by a mechanical (or viscoelastic) model based on two springs and a dashpot, commonly called standard-linear solid, whose parameters depend on the thermal properties and a relaxation time, and yield the isothermal and adiabatic velocities at the low- and high-frequency limits. This model differs from the more general Lord-Shulman theory of thermoelasticity, whose low-frequency velocity is the adiabatic one. These theories are the basis of thermoelastic attenuation in inhomogeneous media, with heterogeneities much smaller than the wavelength, such as Savage's theory of thermoelastic dissipation in a medium with spherical pores. In this case, the shape of the relaxation peak differs from that of the Zener and Lord-Shulman models. In these effective homogeneous media, the anelastic behavior of real materials can better be described by using a stress-strain relation based on fractional derivatives. In particular, wave propagation (dispersion and attenuation) is well described by a Cole-Cole stress-strain equation, as illustrated by the agreement with Savage's theory. We propose a time-domain algorithm based on the Grünwald-Letnikov numerical approximation of the fractional time derivative involved in the time-domain representation of the Cole-Cole model. The spatial derivatives are computed with the Fourier pseudospectral method. We verify the results by comparison with the analytical solution, based on the Green function. The numerical example illustrates wave propagation at an interface separating a porous medium and a purely solid phase.

ARTICLE HISTORY
Received 18 November 2019
Accepted 16 January 2020

KEYWORDS
Zener model; Lord-Shulman model; Cole-Cole model; thermoelasticity; attenuation; fractional derivatives; wave simulation

1. Introduction

Heat diffusion is one of the loss mechanism to explain the behavior of anelastic wave propagation. The theory to describe this behavior is thermoelasticity, i.e., the heat equation coupled with the theory of dynamic elasticity, based on the relation between the fields of stress-strain and temperature [1–6]. Basically, mechanical and/or heat sources induce a temperature field and the heat current equalizes the temperature difference with the surroundings giving rise to energy dissipation. An analysis of the physics of plane waves has been developed by [7], which is a generalization of the energy balance for the isothermal case [e.g., 8]. P and S wave energies are lost because of thermal diffusion. In inhomogeneous media, the existence of a thermal mode, diffusive at low frequencies and wave-like at high frequencies, induces more dissipation [3, 9, 10]. For instance, if the matrix porosity varies significantly from point to point, there is additional loss due to P wave

CONTACT Jing Ba jba@hhu.edu.cn School of Earth Sciences and Engineering, Hohai University, Nanjing, China.

to thermal-wave conversion, which can be termed wave-induced thermoelastic attenuation in analogy with wave-induced fluid-flow attenuation caused by the Biot slow mode in porous media [e.g., 8, 11].

Ref. [12] developed a theory based on the standard-linear-solid mechanical model (or Zener model in viscoelasticity) by introducing a relaxation time into the equations of thermoelasticity. This approach describes the attenuation of the P waves. On the other hand, [13] considered a more general (physical) system of equations (compared to those of [1, 14] and [2]), based on a hyperbolic heat-transfer equation, which also contains a relaxation term (LS theory), that can basically be related to the Maxwell mechanical model. A physical justification is given by [15–18]. Ref. [9] implemented this theory in numerical modeling of wave propagation, whereas [10] solved the poro-thermoelastic case. The differential equations include as solution the thermal wave having similar characteristics to the fast and slow P waves of poroelasticity [19]. Ref. [20] considers the LS lattice model, based on the Debye theory [21], by which heat is transported by elastic waves (phonons) in a crystal lattice (it holds for dielectrics, not metals). It follows that the velocity of the thermal wave must be less or equal to the isothermal P-wave velocity [9, 22].

Many authors have used fractional calculus as an empirical tool to describe the properties of linear viscoelastic materials [e.g., 23–25]. A wide bibliography up to nowadays is contained in the recent book by [26] including an historical perspective up to the 1980's. Ref. [27] reviews methods for fractional-order problems and provides a set of MATLAB routines. Fractional derivatives have been used in thermoelasticity, mostly based on the Caputo derivative [e.g., 28–30]. This derivative [31, 32] is an analytical tool to solve fractional differential equations, and is approximated here with the numerical Grünwald-Letnikov (GL) derivative. The book by [33] reviews the theoretical aspects in the field of fractional thermoelasticity. The Cole-Cole model has been used to describe attenuation by [34] who performed experiments at frequencies from 4 to 400 Hz in fluid-saturated sandstones and limestones, implying a stress-relaxation mechanism in the presence of pore fluids. Ref. [35] simulated wave propagation in viscoelastic media using the Cole-Cole model and fractional time derivatives. An optimal fit of electromagnetic experimental data has been obtained with the Cole-Cole model [8, 36; eq. (8.138)]. Refs. [37, 38] and [39] solved the electromagnetic equations using dissimilar techniques to compute the fractional derivative. Ref. [40] suggest the use of the Cole-Cole model to propagate waves in blood in the context of thermoelasticity and homogeneous media. Here, we show that the model can be linked to a physical process such as wave-induced thermal flow.

Following [41] [Eq. (24)], the heat equation can be generalized so that the relaxation due to the heat diffusion is governed by a fractional differential equation [see also [26], Eq. (3.48)]. We propose to solve the [12] time-domain differential equations based on the Cole-Cole model with a direct method, where the spatial derivatives are computed by using the staggered Fourier pseudospectral method [e.g., 8]. Fractional time derivatives are computed with the GL approximation [42, 43], which is an extension of the standard finite-difference approximation for derivatives of integer order. Moreover, we show that the Q factor of the P wave in [13] theory can be well approximated by the Zener mechanical model [12].

The paper is organized as follows. First, we establish the Zener and Lord-Shulman thermoelasticty equations. Second, we present the Cole-Cole model in the frequency and time domains. Then, we illustrate the numerical algorithm to discretize the differential equations. Finally, we test the model with an analytical solution and present results for the case of a medium with empty spherical pores.

2. Zener and Lord-Shulman thermoelasticity equations

Let us define by σ the stress field, and by T the increment of temperature above a reference absolute temperature T_0 for the state of zero stress and strain. In a linear isotropic medium, the

stress-strain relations of thermoelasticity describing P waves is given by [14, Eq. (2.2)]

$$\sigma = P_0\epsilon - \beta T \tag{1}$$

where ϵ is the trace of the strain tensor, P_0 is the isothermal P-wave modulus and β is the thermal expansion [e.g., 9]. This quantity is usually expressed as $\beta = 3\alpha K$, where α is the coefficient of linear thermal expansion (the volumetric one is 3α), and K is the isothermal bulk modulus. Moreover $P_0 = K + 4\mu/3$, where μ is the isothermal shear modulus.

On the other hand, the law of heat conduction is

$$\gamma\nabla^2 T = c\dot{T} + \beta T_0\dot{\epsilon} \tag{2}$$

[44, Eq. (32.2); 26, Eq. (3.43)], where γ is the coefficient of heat conduction (or thermal conductivity), c is the volumetric specific heat coefficient, ∇^2 is the Laplacian, and a dot above a variable denotes time derivative.

2.1. Zener equations

Ref. (12) replaces the term containing the Laplacian in Eq. (2) by a relaxation term [see p. 77, Eqs (117) and (122)]. His solutions satisfy

$$\frac{\gamma}{c}\nabla^2 T + {\tau_\sigma}^{-1} T = 0, \tag{3}$$

where τ_σ is a relaxation time. It can be shown that with this assumption, the heat equation (2) becomes a memory-variable equation equivalent to that of viscoelasticity [e.g., 8], with T being the memory (or hidden) variable. Substituting Eq. (3) into (2) yields

$$\dot{T} = -\tau_\sigma^{-1} T - \frac{\beta}{c} T_0\dot{\epsilon}. \tag{4}$$

Combining Eqs. (1) and (4), we obtain

$$\sigma + \tau_\sigma\dot{\sigma} = P_0(\epsilon + \tau_\epsilon\dot{\epsilon}), \tag{5}$$

which is the classical Zener model [e.g., 8], where

$$\tau_\epsilon = \left(\frac{c_A}{c_I}\right)^2 \tau_\sigma, \tag{6}$$

$$c_I = \sqrt{\frac{P_0}{\rho}} \text{ and } c_A = \sqrt{c_I^2 + b^2} \tag{7}$$

are the isothermal and adiabatic velocities, respectively,

$$b = \beta\sqrt{\frac{T_0}{\rho c}} \tag{8}$$

and ρ is the mass density. The unrelaxed (adiabatic) P-wave modulus is

$$P_\infty = \left(\frac{c_A}{c_I}\right)^2 P_0. \tag{9}$$

Neglecting inertial terms [14, Eq. (10.1)], the stress-equilibrium equation implies $\nabla\cdot\sigma = 0$, and taking the gradient in Eq. (1) gives $P_0\nabla^2\epsilon = \beta\nabla^2 T$, which combined with Eq. (2) gives the following diffusion equation

$$\dot{\mathcal{T}} = D\nabla^2\mathcal{T}, \text{ with } \mathcal{T} = \nabla^2 T. \tag{10}$$

where

$$D = \left(\frac{c_I}{c_A}\right)^2 a^2, \text{ with } a^2 = \frac{\gamma}{c}, \tag{11}$$

is the corresponding thermal diffusivity.

Appendix A presents a plane-wave analysis of the thermoelastic equations, where

$$Q_0 = \frac{2\sqrt{P_\infty P_0}}{P_\infty - P_0} = \frac{2\sqrt{P_\infty/P_0}}{P_\infty/P_0 - 1} = \frac{2\sqrt{\gamma/(cD)}}{\gamma/(cD) - 1} \tag{12}$$

and

$$\tau_\sigma = \frac{1}{2\pi f_0}\sqrt{\frac{cD}{\gamma}} = \frac{1}{2\pi f_0}\cdot\frac{c_I}{c_A}. \tag{13}$$

Hence, given the location of the thermoelastic peak, f_0, the thermal properties, γ, c and D and the isothermal modulus, P_0, the wave properties are fully defined.

2.2. Lord-Shulman equations

The LS thermoelasticity dispersion equation refers to [20, 45] and [9]. We outline in Appendix A a plane-wave analysis based on the LS theory and implemented by [9] in numerical modeling of wave propagation. Ref. [10] generalized this approach to the poro-thermoelastic case.

It is clear from the previous section and Appendix A that the low- and high-frequency velocities of the Zener theory are c_I and c_A, respectively, while those of the LS theory are c_A and c_∞, where

$$c_\infty = \frac{1}{2}\sqrt{c_A^2 + c_I^2 + \sqrt{(c_A^2 + c_I^2)^2 - 4c_I^4}} \tag{14}$$

[this velocity is based on Eq. (7), lattice model]. This also implies a different level of attenuation as we shall see in the examples. The Zener and Cole-Cole models are adapted to match these more realistic velocities, such that

$$\tau_\epsilon = \left(\frac{c_\infty}{c_A}\right)^2 \tau_\sigma \text{ and } P_\infty = \left(\frac{c_\infty}{c_A}\right)^2 P_0, \tag{15}$$

instead of Eqs. (6) and (9), respectively.

3. The Cole-Cole model

Effective attenuation can be described by means of power laws in the form of fractional derivatives. A generalization of the thermoelastic equation can be achieved by using the Cole-Cole model [8, 36, 41, 43, 46, 47], which involves derivatives of fractional order and is used to describe dispersion and energy loss in dielectrics, anelastic media and electric networks. The complex modulus of a Cole-Cole element generalizes Eq. (33) to

$$P(\omega) = P_0 \cdot \frac{1 + (\mathrm{i}\omega\tau_\epsilon)^q}{1 + (\mathrm{i}\omega\tau_\sigma)^q} \tag{16}$$

Refs. [8, 41], where $0 \leq q < 2$ is a real number, and the relaxation times are given by Eq. (34). The quality factor has a minimum value located at f_0, as in the Zener case. The unrelaxed modulus is $P_\infty = P_0(\tau_\epsilon/\tau_\sigma)^q$. The peak dissipation factor (Q^{-1}) depends on q, and when $q = 1$, we

obtain the Zener model. This additional parameter is closely related to the width of the relaxation peak and allows us to fit realistic attenuation levels.

In order to fit experimental data, one requires a parameterization with f_0, Q_0 and q, since the peak dissipation factor Q_0 and the location of the peak are generally reported in the literature [e.g., 3]. In this case, the relaxation times depend on q and the peak dissipation factor is the same regardless the value of q. The relaxation times are

$$\tau_\epsilon = \frac{\kappa^{1/q}}{2\pi f_0}, \quad \tau_\sigma = \frac{\kappa^{-1/q}}{2\pi f_0}, \tag{17}$$

where

$$\kappa = \frac{1 + \sqrt{1 + Q_0^2}\sin\varphi}{Q_0 \sin\varphi - \cos\varphi}, \quad \varphi = \frac{\pi q}{2} \tag{18}$$

[48].

The Cole-Cole model stress (σ)-strain (ϵ) relation, corresponding to the modulus (16), is [41]

$$\sigma + \tau_\sigma^q \frac{\partial^q \sigma}{\partial t^q} = P_0 \left(\epsilon + \tau_\epsilon^q \frac{\partial^q \epsilon}{\partial t^q} \right) \tag{19}$$

The limit $\tau_\epsilon = 0$ gives the Kelvin-Voigt model implemented in [43]. In the frequency domain, we have

$$\sigma = P\epsilon. \tag{20}$$

4. 2D Wave equation

The conservation of linear momentum for a 2 D linear thermoelastic medium, describing dilatational deformations, can be written as

$$\rho \ddot{u}_i = \partial_i \sigma, \;\; i = 1(x), 2(y) \tag{21}$$

[e.g., 8], where u_i are displacement components and ∂_i denotes spatial derivatives.

The initial conditions are $u_i(0, \mathbf{x}) = 0, \partial_t u_i(0, \mathbf{x}) = 0,$ and $u_i(t, \mathbf{x}) = 0,$ for $t < 0$, where $\mathbf{x}$ is the position vector. The strain-displacement relation is $\epsilon = \partial_1 u_1 + \partial_2 u_2$. Then, the complete set of equations describing the propagation is

$$\begin{aligned} \ddot{u}_1 &= \rho^{-1} \partial_1 \sigma, \\ \ddot{u}_2 &= \rho^{-1} \partial_2 \sigma, \\ \sigma + \tau_\sigma^q \frac{\partial^q \sigma}{\partial t^q} &= P_0 \left(\epsilon + \tau_\epsilon^q \frac{\partial^q \epsilon}{\partial t^q} \right), \\ \epsilon &= \partial_1 u_1 + \partial_2 u_2. \end{aligned} \tag{22}$$

5. Numerical algorithm

The calculation of a fractional derivative is based on the Grünwald-Letnikov (GL) approximation, such that for a function g it is

$$\frac{\partial^q g}{\partial t^q} \approx D^q g = \frac{1}{h^q} \sum_{j=0}^{J} (-1)^j \binom{q}{j} g(t - jh), \tag{23}$$

where h is the time step, and $J = t/h - 1$. The derivation of this expression can be found, for instance, in [42]. The binomial coefficients are negligible for j exceeding an integer J, the effective memory length. When $q < 1$, the decay of the binomial coefficients is slow [e.g., 42, 49], and J is large. Then, we increase the order of the derivative by applying a time derivative of order m to the third Eq. (22). The result is

$$\begin{aligned}
&\partial_t^2 u_1 = \rho^{-1}\partial_1\sigma,\\
&\partial_t^2 u_2 = \rho^{-1}\partial_2\sigma,\\
&D^m\sigma + \tau_\sigma^q D^{m+q}\sigma = P_0(D^m\epsilon + \tau_\epsilon^q D^{m+q}\epsilon) + s,\\
&\epsilon = \partial_1 u_1 + \partial_2 u_2.
\end{aligned} \tag{24}$$

where we added a source term s. It is enough to take $m = 1$ to have a considerable saving in memory storage compared to $m = 0$.

Discretizing Eq. (24) as $t = nh$ and defining $u^n = u(nh)$, the left-hand side of the first two equations of equations (24) can be written as

$$h^2(D^2 u_i)^n = u_i^{n+1} - 2u_i^n + u_i^{n-1}, i = 1, 2, \tag{25}$$

where we have used a right-shifted finite-difference expression for the second derivative. The third equation is

$$\sigma^n = P_0(\epsilon^n + \Sigma_\epsilon + h^m\tau_\epsilon^q D_\epsilon^{q+m}) - \Sigma_\sigma - h^m\tau_\sigma^q D_\sigma^{q+m} \tag{26}$$

with

$$\Sigma_\xi = \sum_{j=1}^{m}(-1)^j\binom{m}{j}\xi^{m-j}, \tag{27}$$

Let us consider the case $m = 1$. The GL derivative of g at time nh can be rewritten as

$$D^{q+1}g^n = \frac{g^n}{h^{q+1}} + r_g^{(q+1)}, r_g^{(q+1)} = \frac{1}{h^{q+1}}\sum_{j=1}^{J}(-1)^j\binom{q+1}{j}g^{n-j}, \tag{28}$$

where $r_g^{(q+1)}$ has the memory of the field from n – 1 back in time.

Then, the final discretized equations are

$$\begin{aligned}
&u_1^{n+1} = h^2(\rho^{-1}\partial_1\sigma^n) + 2u_1^n - u_1^{n-1},\\
&u_2^{n+1} = h^2(\rho^{-1}\partial_2\sigma^n) + 2u_2^n - u_2^{n-1},\\
&\sigma^n = \frac{1}{a_\sigma}[\sigma^{n-1} - h\tau_\sigma^q r_\sigma^{q+1} + P_0(a_\epsilon\epsilon^n - \epsilon^{n-1} + h\tau_\epsilon^q r_\epsilon^{q+1}) + hs^n],\\
&\epsilon^n = \partial_1 u_1^n + \partial_2 u_2^n,
\end{aligned} \tag{29}$$

where

$$a_\xi = 1 + \left(\frac{\tau_\xi}{h}\right)^q, \xi = \epsilon, \sigma. \tag{30}$$

The spatial derivatives are calculated with the staggered Fourier method, which has spectral accuracy for band-limited signals [8, 49, 50], so that the results have not spatial numerical dispersion. Since we use Fourier basis functions to compute the spatial derivatives, Eq. (29) satisfy periodic boundary conditions at the edges of the numerical mesh.

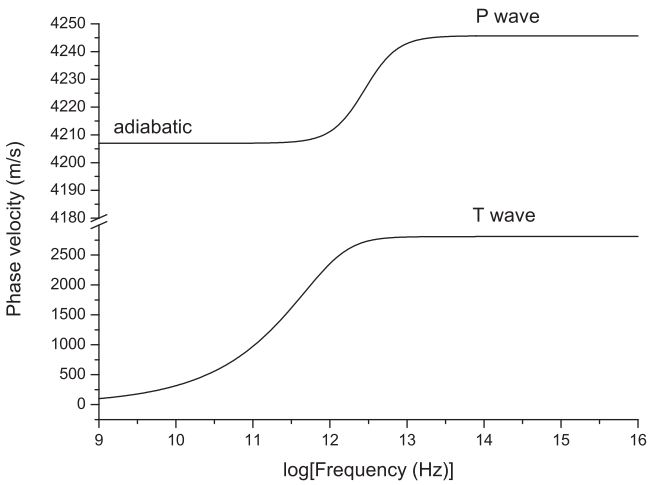

Figure 1. Phase velocities of the P and T waves corresponding to the Lord-Shulman theory of thermoelasticity.

6. Results

We define the Grüneisen ratio [51],

$$\Gamma = \frac{\beta}{c} \tag{31}$$

(dimensionless). Let us consider the following typical properties of a sandstone:

density, ρ : 2600kg/m^3
Grüneisen ratio, Γ : 1.1
Volumetric specific heat, c : 2.8×10^6 kg/(m s$^{2^\circ}$K)
thermal conductivity , γ : 2.3 m kg/(s$^{3^\circ}$K)
isothermal P − wave velocity, $c_I = \sqrt{P_0/\rho}$: 4160 m/s
absolute temperature, T_0 : 300°K,
relaxation time, $\tau = 10^{-13}$ s = 0.1 ps,

where we have expressed the quantities in the international systems of units (SI). These values yield $P_0 = 45$ GPa, $a^2 = 8.2 \times 10^{-7}$ m^2/s, $b = 625$ m/s, $c_A = 4207$ m/s, $c_\infty = 4245$ m/s and $c_{T\infty} = 2808$ m/s (see Figure 1). The relaxation time can be chosen with the criteria indicated by [20] [see Eq. (42) in Appendix A]. Here we take a higher value (0.1 ps against 0.05 ps). As τ decreases the attenuation and dispersion increase, and generally, the attenuation of the P wave at seismic frequencies is negligible in homogeneous media. However, in the presence of heterogeneities and/or cracks or cavities, much smaller than the signal wavelength, the conversion of T diffusion mode to P wave generates attenuation at low frequencies. This process is similar to wave-induced fluid-flow attenuation [e.g., 11], by which P-wave to slow P (Biot)-wave conversion is the main physical mechanism.

The LS theory predicts two compressional waves, namely the P and T waves, the latter commonly termed the second sound wave [52]. The phase velocities are shown in Figure 1, where the T-wave mode is diffusive at low frequencies with a very high dissipation factor, orders of magnitude larger that that of the P wave. Figure 2 compares the Zener and LS phase velocities and quality factors. As can be seen, the Zener thermoelastic model predicts a higher attenuation, a result of the stronger velocity dispersion, according to the Kramers-Kronig relations, and lower velocities. The dotted line is a fit of the LS curves with the Zener mechanical model. Since the agreement is very good, the LS model satisfies the relations [53]. Then, we can use the Zener

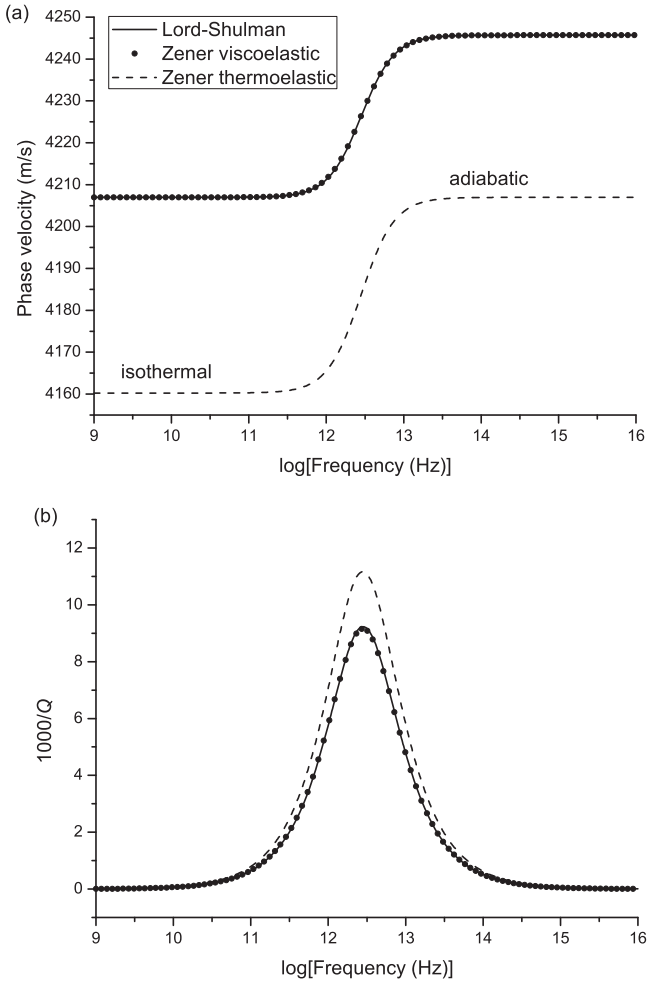

Figure 2. Comparison between the Zener and Lord-Shulman theories of thermoelasticity: Phase velocity (a) and dissipation factor (b) of the P wave. The symbols represent a fit with the Zener (standard-linear solid) mechanical model.

mechanical model and its generalization (Cole-Cole model) adapted to match the more realistic velocities predicted by the LS theory.

Figure 3 shows the Cole-Cole phase velocity (a) and dissipation factor (b) as a function of frequency for three values of the order q, where $q=1$ is the Zener model. The thermoelastic medium corresponds to the above properties, whose Zener parameters are $P_\infty = 47$ GPa, $f_0 = 2810$ GHz, $Q_0 = 50$, $\tau_\epsilon = 0.058$ ps and $\tau_\sigma = 0.055$ ps, so that the high-frequency modulus has the same value. The low-frequency stiffnesses P_0 are 45.36, 45 and 44.63 GPa for $q=0.8$, 1, and 1.2, respectively. The peak attenuation and the velocity dispersion increase with increasing q.

On the other hand, using the parameterization (17)-(18), the peak dissipation factor is constant, regardless the value of q and the relaxation times vary with q. An example is illustrated in [48].

Now, we consider the thermoelastic model developed by [3] for a porous medium with spherical pores of radius R (see Appendix B). In this case, we have significant attenuation at the seismic band. We assume $R=0.4$ mm, $P_0=\bar{E} = 70$ GPa, $\sigma=0.170$, $\bar{\sigma} = 0.173$, $E=83$ GPa, $K=39$ GPa, $\mu=33$ GPa, $\bar{K} = 33$ GPa, $\bar{\mu} = 27.6$ GPa, $\rho=2600$ kg/m^3, $\phi = 9.54\%$, $\Gamma=1.1$, $\beta=117\times10^6$ kg/(m s^2 $^\circ$ K), $\gamma=532$ m kg/(s^3 $^\circ$ K) and $T_0 = 300$ $^\circ$ K (a barred quantity corresponds to the medium including the pore space). Figure 4 shows the good fit with the Cole-Cole

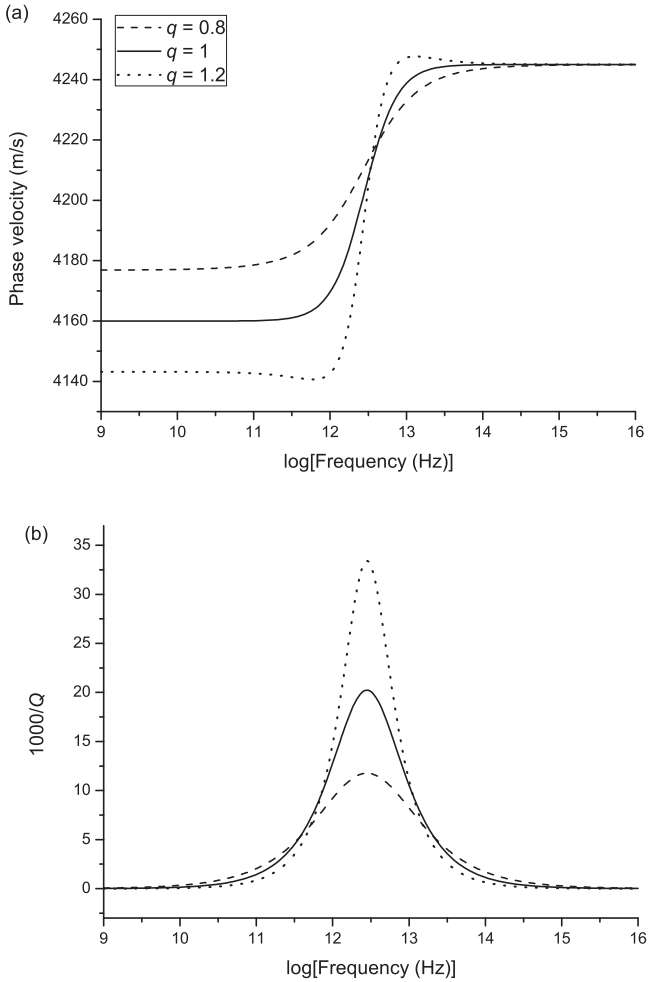

Figure 3. Cole-Cole phase velocity (a) and dissipation factor (b) of the P wave as a function of frequency for different values of the order q ($q = 1$ corresponds to the Zener viscoelastic model of Figure 1).

model based on Eqs. (17)-(18), where we have used $f_0 = 23.37$ Hz, $Q_0 = 35.37$ and $q = 0.82$. The Zener curve is also shown, but only can match the maximum value and the location of the peak. Decreasing γ shifts the relaxation peak to lower frequencies, but the peak dissipation (Q^{-1}) is the same.

We verify the numerical algorithm by comparing numerical and analytical solutions in homogeneous media, where the latter is given in Appendix C. The time history of the source is

$$s(t) = \left(o - \frac{1}{2}\right)\exp(-o), o = \left[\frac{\pi(t - t_s)}{t_p}\right]^2, \tag{32}$$

where t_p is the period of the wave and we take $t_s = 1.4t_p$. The peak frequency is $f_p = 1/t_p$.

The numerical mesh has uniform vertical and horizontal grid spacings of 20 m, and 231×231 grid points. The medium properties are those of the previous example. A dilatational source is applied at the center of the mesh with a peak frequency equal to the relaxation frequency. We use a memory length $L = 75$ and a time step $h = 0.5$ ms. Figure 5 compares the numerical and analytical transient solutions at a distance of $\sqrt{2} \cdot 800$ m from the source location. The agreement between solutions has an L^2- norm error less than 0.5%. A comparison between the lossy and

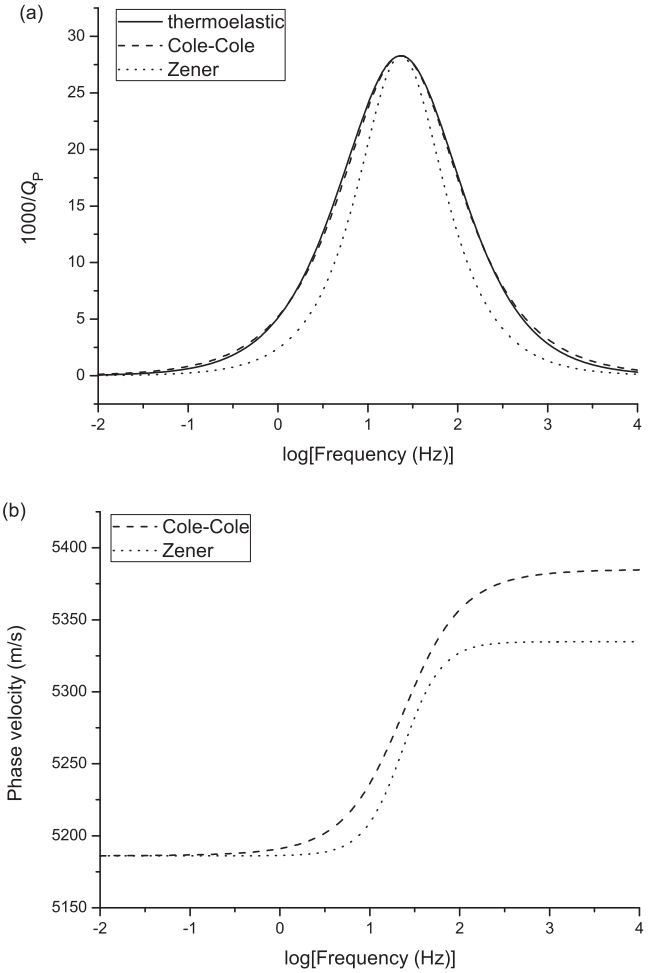

Figure 4. Dissipation factor (a) and phase velocity (b) of thermoelastic [3] model, compared to those of the Cole-Cole and Zener models.

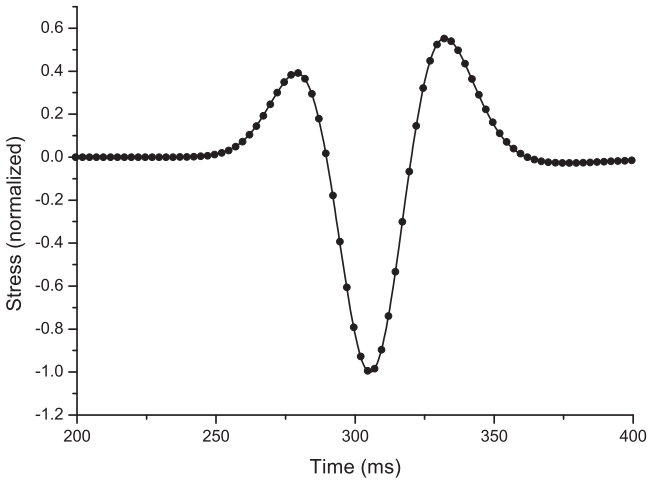

Figure 5. Comparison between the analytical (solid line) and numerical (dots) solutions in a lossy medium.

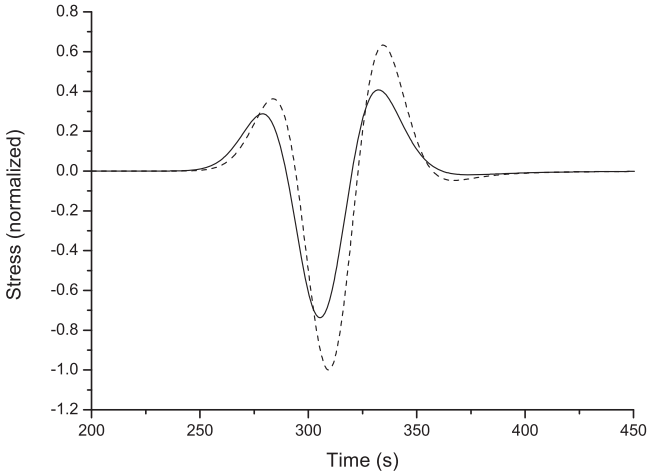

Figure 6. Comparison between the lossy (solid line) and lossless (dashed line) solutions.

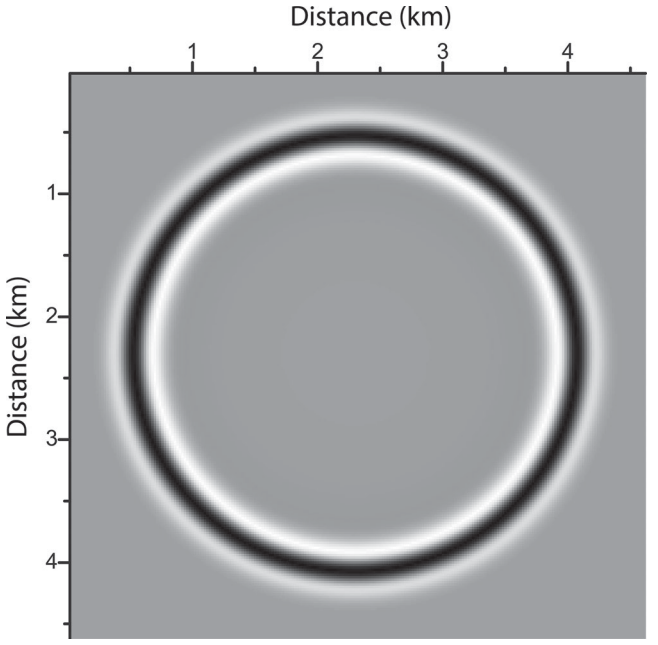

Figure 7. Homogeneous medium. Snapshot of the stress at 450 ms.

lossless ($Q_0 = \infty$) solutions are displayed in Figure 6. Since the elastic (lossless) limit is taken at the low-frequency limit, this pulse is slower than the viscoelastic one. The numerical algorithm allows us to compute snapshots of the wavefield in order to see its evolution. Figure 7 shows a snapshot of the stress field at 450 ms.

Let us consider an inhomogeneous medium, specifically, an interface separating two half-spaces. The upper medium has the properties corresponding to Figure 4, while the lower one has no pores, with $P_0 = E = 170\,\text{GPa}$ and $\rho = 2800\,\text{Kg/m}^3$, i.e., lossless. The upper medium has relaxed and unrelaxed velocities of 5189 and 5388 m/s, while the lower medium has a velocity of 7792 m/s over all the frequency range. Figure 8 shows a snapshot at 350 ms. A weak reflected wave and a strong transmitted wave can be observed.

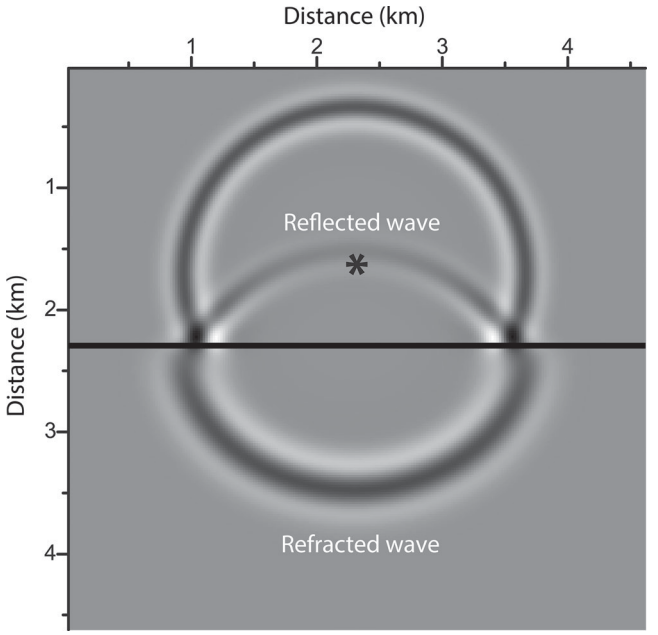

Figure 8. Snapshot of the stress at 350 ms in a inhomogeneous medium. The reflected and transmitted waves are indicated, and the asterisk marks the source location.

7. Conclusions

The classical Zener model of thermoelasticity has been compared to the more general Lord-Shulman theory, whose low-frequency phase velocity is the adiabatic one, while the first has velocities ranging between the isothermal and adiabatic limits. Then, we present a numerical algorithm to model thermoelastic propagation based on the Cole-Cole model, which implies the solution of fractional time derivatives of stress and strain. The kernel of this relation has three parameters that can be obtained by fitting real or synthetic data, namely, the relaxed (low-frequency) velocity, the maximum dissipation factor and the fractional order. We fit the quality factors obtained for homogeneous media and from Savage's theory of thermoelastic loss in porous media. The wave field is computed in the time-space domain using the Grünwald-Letnikov approximation and the staggered Fourier pseudospectral method. The modeling algorithm has been tested with the analytical Green's function.

Appendix: A Plane-wave analysis

A.1. Zener theory and mechanical viscoelastic model

The complex modulus of the Zener model is obtained by taking a time Fourier transform in Eq. (5),

$$P = \frac{\sigma}{\epsilon} = P_0 \cdot \frac{1 + \mathrm{i}\omega\tau_\epsilon}{1 + \mathrm{i}\omega\tau_\sigma} \tag{33}$$

where $\omega = 2\pi f$ is the angular frequency and $\mathrm{i} = \sqrt{-1}$. Setting

$$\tau_\epsilon = \frac{1}{2\pi f_0 Q_0}\left(\sqrt{Q_0^2 + 1} + 1\right) \text{ and } \tau_\sigma = \frac{1}{2\pi f_0 Q_0}\left(\sqrt{Q_0^2 + 1} - 1\right), \tag{34}$$

Eq. (33) can be re-written as

$$P(f) = \frac{Q_0 + \mathrm{i}(f/f_0)(R+1)}{Q_0 + \mathrm{i}(f/f_0)(R-1)} \cdot P_0, R = \sqrt{1 + Q_0^2}, \tag{35}$$

where f_0 is the relaxation frequency, Q_0 is the minimum quality factor at $f_0 = 1/\left(2\pi\sqrt{\tau_\epsilon \tau_\sigma}\right)$, P is the zero-frequency modulus, and f is the frequency.

The unrelaxed modulus ($f \to \infty$) is $P_\infty = [(R+1)/(R-1)]P_0$, and the following relations holds, $Q_0 = 2\sqrt{P_\infty P_0}/(P_\infty - P_0)$, so that the modulus dispersion $P_\infty - P_0$ can approximately be obtained from Q_0. The Zener Q factor is

$$Q_Z = \frac{\mathrm{Re}(P)}{\mathrm{Im}(P)} \tag{36}$$

[e.g., 8], and the phase velocity is

$$c_p = \left[\mathrm{Re}\left\{\frac{1}{v}\right\}\right]^{-1}, v = \sqrt{\frac{P}{\rho}}, \tag{37}$$

where v is the complex velocity and ρ is the mass density [e.g., 8].

Equation (33) is also the mathematical expression of the standard-linear solid mechanical model of viscoelasticity made of springs and dashpots, also called Zener viscoelastic model [e.g., 8]. In this case, the relaxation times depend on the viscosity, η, of the dashpot as

$$\tau_\sigma = \left(1 - \frac{P_0}{P_\infty}\right)\tau_\epsilon \text{ and } \tau_\epsilon = \frac{\eta}{P_\infty}. \tag{38}$$

A.2. Lord and Shulman (LS) theory

According to [20] and [9], the dispersion relation is

$$v^4 - (c_A^2 + M)v^2 + Mc_I^2 = 0, M = \frac{\mathrm{i}\omega a^2}{1 + \mathrm{i}\omega\tau}, \tag{39}$$

where τ is a relaxation time. Equation (39) is equivalent to Eq. (39) of [20], which is derived from his Eq. (36) (a factor c_A^4 is missing in the last term of this equation). If $\tau = 0$, we obtain Eq. (9) of [45]. High and low values of τ correspond to peak locations of the P wave, f_p, at low and high frequencies, respectively, with

$$f_p \approx \frac{1}{2\pi\tau}. \tag{40}$$

Equation (39) has the solutions:

$$2v^2 = c_A^2 + M \pm \sqrt{(c_A^2 + M)^2 - 4Mc_I^2}. \tag{41}$$

There are two P-wave solutions, an elastic P wave (plus sign) and a thermal T wave (minus sign). At $\omega = 0$ we have two real solutions: $v = 0$ (T wave) and $v = c_A$ (P wave), independent of τ. If $\tau = 0$, $v = \infty$ (P wave) and $v = v_I$ (T wave) at infinite frequencies.

Ref. [20] takes

$$\tau = \frac{a^2}{c_I^2} \tag{42}$$

for his lattice model [see his Eqs. (34), (37) and (58)]. For $\omega \to \infty$, we have $M \to a^2/\tau = c_I^2$ and the solution is

$$2v^2 = c_A^2 + c_I^2 \pm \sqrt{(c_A^2 + c_I^2)^2 - 4c_I^4}, \tag{43}$$

where the plus and minus signs correspond to the P and T waves, respectively. Denoting the velocities by c_∞ and $c_{T\infty}$, respectively, we have $c_{T\infty} < c_I < c_A < c_\infty$. The relaxed and unrelaxed P-wave moduli of the LS model – with the choice [29] – are

$$P_0 = \rho c_A^2 \text{ and } P_\infty = \frac{\rho}{2}\left[c_A^2 + c_I^2 + \sqrt{(c_A^2 + c_I^2)^2 - 4c_I^4}\right], \tag{44}$$

respectively.

B. Thermoelastic attenuation of a medium with spherical pores

Ref. [3] obtained the quality factor of the P waves for media filled with spherical pores of radius R. A shear strain produces a dilatation in the cavities, which in turn generates a heat current and a temperature field T. The expression of the dissipation factor is

$$Q_P^{-1}(\omega) = 120 \cdot \frac{1-2\bar{\sigma}}{1-\bar{\sigma}} \cdot \frac{\epsilon\phi\beta^2 T_0}{cK_0} \cdot \frac{(1-2\sigma)(1+\sigma)}{7-5\sigma} F(\omega), \tag{45}$$

where

$$K_0 = \left(1 - \frac{2}{3} \cdot \frac{2\sigma-1}{\sigma-1}\right) P_0, \epsilon = 1 + \frac{15\phi(1-\sigma)}{7-5\sigma}, \tag{46}$$

$$\begin{aligned} F(\omega) &= \frac{\chi^2(2\chi^2+5\chi+4)}{\left[(2\chi^3-9\chi-9)^2+\chi^2(2\chi^2+8\chi+9)^2\right]}, \\ \chi &= \sqrt{\frac{\omega}{2}} \cdot \frac{R}{a}, \end{aligned} \tag{47}$$

where σ and $\bar{\sigma}$ are the relaxed Poisson ratio of the mineral and porous medium (at zero frequency), respectively, and ϕ is the porosity.

C. Green's function and analytical solution

We obtain a 2 D analytical solution of Eqs. (24) with $m = 1$ in homogeneous media. Combining the equations, we have

$$\ddot{\epsilon} = \frac{1}{\rho}\Delta\sigma. \tag{48}$$

Using Eqs. (2), (20) and (24), Eq. (48) becomes a Helmholtz equation in the frequency domain,

$$\Delta\epsilon + k^2\epsilon = -\frac{\Delta s}{\mathrm{i}\omega P\left[1+(\mathrm{i}\omega\tau_\sigma)^q\right]}, k = \frac{\omega}{v}, \tag{49}$$

where k is the wavenumber and v is given by Eq. (37). If v is real, the medium is lossless. The solution to the acoustic (lossless) equation $(\Delta + k^2)G = -8\delta(r)$ is the Green function $G = -2\mathrm{i}H_0^{(2)}(kr)$, with $v = c_a$ (the acoustic velocity), where $H_0^{(2)}$ is the zero-order Hankel function of the second kind [e.g., 8]. More precisely,

$$G(x, y, x_0, y_0, \omega, c_a) = -2\mathrm{i}H_0^{(2)}\left(\frac{\omega r}{c_a}\right) \tag{50}$$

where (x_0, y_0) is the source location, and

$$r = \sqrt{(x-x_0)^2 + (y-y_0)^2}. \tag{51}$$

The anelastic solution is obtained by invoking the correspondence principle [8], i.e., by substituting the acoustic velocity c_a with the complex velocity v. The differential operator $-\Delta/(\mathrm{i}\omega P[1+(\mathrm{i}\omega\tau_\sigma)^q])$ acts on the source in Eq. (49). Thus, the Green function for the strain is

$$G_\epsilon = -\frac{1}{\mathrm{i}\omega P\left[1+(\mathrm{i}\omega\tau_\sigma)^q\right]}\Delta G. \tag{52}$$

Since $\Delta G = -p^2 G$ away from the source and using Eq. (20), the Green function for the stress is

$$G_\sigma = PG_\epsilon = \frac{k^2 G}{\mathrm{i}\omega\left[1+(\mathrm{i}\omega\tau_\sigma)^q\right]}. \tag{53}$$

We set $G(-\omega) = G^*(\omega)$, where the superscript "*" denotes complex conjugation. This equation ensures that the inverse Fourier transform of the Green's function is real. The frequency-domain solution is then given by $\sigma(\omega) = \frac{1}{8}G_\sigma(\omega)F(\omega)$, where F is the Fourier transform of the source time history. Hence,

$$\sigma(x, y, x_0, y_0, \omega) = \frac{1}{8}G_\sigma F = -\frac{\omega F(\omega)}{4v^2\left[1+(\mathrm{i}\omega\tau_\sigma)^q\right]} H_0^{(2)}\left(\frac{\omega r}{v}\right), \tag{54}$$

Because the Hankel function has a singularity at $\omega = 0$, we assume $G = 0$ for $\omega = 0$, an approximation that does not have a significant effect on the solution (note, moreover, that $F(0) = 0$). The time-domain solution $\sigma(t)$ is obtained by a discrete inverse Fourier transform. We have tacitly assumed that σ and $\dot{\sigma}$ are zero at time $t = 0$.

Funding

This work is supported by the Specially-Appointed Professor Program of Jiangsu Province, China, the Jiangsu Province Innovation and Entrepreneurship Plan of China, and the National Natural Science Foundation of China (grant no. 41974123).

References

[1] C. Zener, "Internal friction in solids. II. General theory of thermoelastic internal friction," *Phys. Rev.*, vol. 53, no. 1, pp. 90–99, 1938. DOI: 10.1103/PhysRev.53.90.
[2] S. Treitel, "On the attenuation of small-amplitude plane stress waves in a thermoelastic solid," *J. Geophys. Res.*, vol. 64, no. 6, pp. 661–665, 1959. DOI: 10.1029/JZ064i006p00661.
[3] J. Savage, "Thermoelastic attenuation of elastic waves by cracks," *J. Geophys. Res.*, vol. 71, no. 16, pp. 3929–3938, 1966. Correction: 1967, JGR, 72, 6387. DOI: 10.1029/JZ072i024p06387-02.
[4] B. H. Armstrong, "Models for thermoelastic in heterogeneous solids attenuation of waves," *Geophysics*, vol. 49, no. 7, pp. 1032–1040, 1984. DOI: 10.1190/1.1441718.
[5] J. L. Wegner, and J. B. Haddow, "Linear thermoelasticity, second sound and the entropy inequality," *Wave Motion*, vol. 18, no. 1, pp. 67–77, 1993. DOI: 10.1016/0165-2125(93)90061-J.
[6] A. N. Norris, "Dynamics of thermoelastic thin plates: A comparison of four theories," *J. Thermal Stresses*, vol. 29, no. 2, pp. 169–195, 2006. DOI: 10.1080/01495730500257482.
[7] N. H. Scott, "Energy and dissipation of inhomogeneous plane waves in thermoelasticity," *Wave Motion*, vol. 23, no. 4, pp. 393–406, 1996. DOI: 10.1016/0165-2125(96)00003-0.
[8] J. M. Carcione, 2014, *Wave Fields in Real Media. Theory and Numerical Simulation of Wave Propagation in Anisotropic, Anelastic, Porous and Electromagnetic Media*, 3rd ed. New York: Elsevier. (extended and revised).
[9] J. M. Carcione, Z.-W. Wang, W. Ling, E. Salusti, J. Ba, and L.-Y. Fu, "Simulation of wave propagation in linear thermoelastic media," *Geophysics*, vol. 84, no. 1, pp. T1–T11, 2018b. DOI: 10.1190/geo2018-0448.1.
[10] J. M. Carcione, F. Cavallini, W. E, Ba, J, and L.-Y. Fu, "Physics and simulation of wave propagation in linear thermo-poroelastic media," *J. Geophys. Res.*, vol. 124, no. 8, pp. 8147–8166, 2019. DOI: 10.1029/2019JB017851.
[11] T. M. Müller, G. Gurevich, and M. Lebedev, "Seismic wave attenuation and dispersion resulting from wave-induced flow in porous rocks – A review," *Geophysics*, vol. 75, no. 5, pp. 75A147–75A164, 2010. DOI: 10.1190/1.3463417.
[12] C. Zener, 1948, *Elasticity and Anelasticity of Metals*. Chicago, IL: The University of Chicago Press.
[13] H. Lord, and Y. Shulman, "A generalized dynamical theory of thermoelasticity," *J. Mech. Phys. Solid*, vol. 15, no. 5, pp. 299–309, 1967. DOI: 10.1016/0022-5096(67)90024-5.
[14] M. A. Biot, "Thermoelasticity and irreversible thermodynamics," *J. Appl. Phys.*, vol. 27, no. 3, pp. 240–253, 1956. DOI: 10.1063/1.1722351.
[15] C. Cattaneo, "Sulla conduzione del calore," *Atti Sem. Mat. e Fis. Univ. Modena*, vol. 3, pp. 13–21, 1948.
[16] W. Dreyer, and H. Struchtrup, "Heat pulse experiments revisited," *Continuum Mech. Thermodyn.*, vol. 5, no. 1, pp. 3–50, 1993. DOI: 10.1007/BF01135371.
[17] R. Peierls, "Zur kinetischen theorie der wärmeleitung in kristallen," *Ann. Phys.*, vol. 3, pp. 1055–1101, 1929. DOI: 10.1002/andp.19293950803.
[18] D. Y. Tzou, "An engineering assessment to the relaxation time in thermal wave propagation," *Int. J. Heat Mass Transf.*, vol. 36, no. 7, pp. 1845–1851, 1993. DOI: 10.1016/S0017-9310(05)80171-1.
[19] M. A. Biot, "Theory of propagation of elastic waves in a fluid-saturated porous solid. I. Low-frequency range," *J. Acoust. Soc. Am.*, vol. 28, no. 2, pp. 168–178, 1956. DOI: 10.1121/1.1908239.
[20] A. J. Rudgers, "Analysis of thermoacoustic wave propagation in elastic media," *J. Acoust. Soc. Am.*, vol. 88, no. 2, pp. 1078–1094, 1990. DOI: 10.1121/1.399856.
[21] C. Kittel, 1956, *Introduction to Solid State Physics*, 2nd ed. New York: Wiley, pp. 125–155.
[22] Z.-W. Wang, L.-Y. Fu, J. Wei, W. Hou, J. Ba, and J. M. Carcione, "On the Green function of the Lord-Shulman thermoelasticity equations," *Geophys. J. Int.*, vol. 220, no. 1, pp. 393–403, 2019. DOI: 10.1093/gji/ggz453.
[23] M. Caputo, and F. Mainardi, "New dissipation model based on memory mechanism," *Pure Appl. Geophys.*, vol. 91, no. 1, pp. 134–147, 1971a. DOI: 10.1007/BF00879562.
[24] M. Caputo, and F. Mainardi, "Linear models of dissipation in anelastic solids," *Riv. Nuovo Cimento (Ser. II)*, vol. 1, no. 2, pp. 161–198, 1971b. DOI: 10.1007/BF02820620.
[25] F. Mainardi, and G. Spada, "Creep, relaxation and viscosity properties for basic fractional models in rheology," *Eur. Phys. J. Special Topics*, vol. 193, no. 1, pp. 133–160, 2011. DOI: 10.1140/epjst/e2011-01387-1.
[26] F. Mainardi, 2010, *Fractional Calculus and Waves in Linear Viscoelasticity*. London: Imperial College Press.

[27] R. Garrappa, "Numerical solution of fractional differential equations: A survey and a software tutorial," *Mathematics*, vol. 6, no. 2, pp. 16, 2018. No DOI: 10.3390/math6020016.
[28] H. H. Sherief, A. M. A. El-Sayed, and A. M. Abd El-Latief, "Fractional order theory of thermoelasticity," *Int. J. Solids Struct.*, vol. 47, no. 2, pp. 269–275, 2010. DOI: 10.1016/j.ijsolstr.2009.09.034.
[29] W. E. Raslan, "Application of fractional order theory of thermoelasticity to a 1D problem for a cylindrical cavity," *Arch. Mech.*, vol. 66, pp. 257–267, 2014.
[30] R. Garra, "Propagation of nonlinear thermoelastic waves in porous media within the theory of heat conduction with memory: Physical derivation and exact solutions," *Math. Methods Appl. Sci.*, vol. 40, no. 4, pp. 1307–1315, 2017. DOI: 10.1002/mma.4055.
[31] M. Caputo, "Linear model of dissipation whose Q is almost frequency independent-II, Geophys," *J. Roy. Astr. Soc.*, vol. 13, no. 5, pp. 529–539, 1967. DOI: 10.1111/j.1365-246X.1967.tb02303.x.
[32] I. Podlubny, 1999, *Fractional Differential Equations*, San Diego, CA: Academic Press.
[33] Y. Povstenko, 2015, *Fractional Thermoelasticity*, New York, NY: Springer.
[34] J. W. Spencer, "Stress relaxations at low frequencies in fluid-saturated rocks: Attenuation and modulus dispersion," *J. Geophys. Res.*, vol. 86, no. B3, pp. 1803–1812, 1981. DOI: 10.1029/JB086iB03p01803.
[35] J.-F. Lu, and A. Hanyga, "Numerical modelling method for wave propagation in a linear viscoelastic medium with singular memory," *Geophys. J. Int.*, vol. 159, no. 2, pp. 688–702, 2004. DOI: 10.1111/j.1365-246X.2004.02409.x.
[36] K. S. Cole, and R. H. Cole, "Dispersion and absorption in dielectrics. I. Alternating current characteristics," *J. Chem. Phys.*, vol. 9, no. 4, pp. 341–351, 1941. DOI: 10.1063/1.1750906.
[37] H. H. Abdullah, H. A. Elsadek, H. E. ElDeeb, and N. Bagherzadeh, "Fractional derivatives based scheme for FDTD modeling of nth-order Cole-Cole dispersive media," *IEEE Antennas Wirel. Propag. Lett.*, vol. 11, pp. 281–284, 2012. DOI: 10.1109/LAWP.2012.2190029.
[38] I. T. Rekanos, and T. V. Yioultsis, "Approximation of Grünwald-Letnikov fractional derivative for FDTD modeling of Cole-Cole media," *IEEE Trans. Magn.*, vol. 2, pp. 7004304, 2014.
[39] P. Bia, D. Caratelli, L. Mescia, R. Cicchetti, G. Maione, and F. Prudenzano, "A novel FDTD formulation based on fractional derivatives for dispersive Havriliak-Negami media," *Signal Process.*, vol. 105, pp. 312–318, 2015. DOI: 10.1016/j.sigpro.2014.05.031.
[40] F. Farsaci, S. Ficarra, A. Galtieri, and E. Tellone, "A new non-equilibrium thermodynamic fractional visco-inelastic model to predict experimentally inaccessible processes and investigate pathophysiological cellular structures," *Fluids*, vol. 2, no. 4, p. 59, 2017. DOI: 10.3390/fluids2040059.
[41] F. Mainardi, "Fractional relaxation in anelastic solids," *J. Alloys Compounds*, vol. 212, pp. 534–538, 1994. DOI: 10.1016/0925-8388(94)90560-6.
[42] J. M. Carcione, F. Cavallini, F. Mainardi, and A. Hanyga, "Time-domain seismic modeling of constant Q-wave propagation using fractional derivative," *Pure Appl. Geophys.*, vol. 159, no. 7-8, pp. 1719–1736, 2002. DOI: 10.1007/s00024-002-8705-z.
[43] M. Caputo, J. M. Carcione, and F. Cavallini, "Wave simulation in biological media based on the Kelvin-Voigt fractional-derivative stress-strain relation," *Ultrasound Med. Biol.*, vol. 37, pp. 996–1004, 2011. DOI: 10.1016/j.ultrasmedbio.2011.03.009.
[44] L. D. Landau, and E. M. Lifshitz, 1970, *Theory of Elasticity*. New York: Pergamon Press.
[45] H. Deresiewicz, "Plane waves in a thermoelastic solid," *J. Acoustic. Soc. Am.*, vol. 29, no. 2, pp. 204–209, 1957. DOI: 10.1121/1.1908832.
[46] R. L. Bagley, and P. J. Torvik, "On the fractional calculus model of viscoelastic behavior," *J. Rheol.*, vol. 30, no. 1, pp. 133–155, 1986. DOI: 10.1122/1.549887.
[47] A. Hanyga, "An anisotropic Cole-Cole model of seismic attenuation," *J. Comput. Acoust.*, vol. 11, no. 01, pp. 75–90, 2003. DOI: 10.1142/S0218396X03001845.
[48] S. Picotti, and J. M. Carcione, "Numerical simulation of wave-induced fluid-flow seismic attenuation based on the Cole-Cole model," *J. Acous. Soc. Am.*, vol. 142, no. 1, pp. 134–145, 2017. DOI: 10.1121/1.4990965.
[49] J. M. Carcione, "Theory and modeling of constant-Q P- and S-waves using fractional time derivatives," *Geophysics*, vol. 74, no. 1, pp. T1–T11, 2009. DOI: 10.1190/1.3008548.
[50] J. M. Carcione, "Staggered mesh for the anisotropic and viscoelastic wave equation," *Geophysics*, vol. 64, no. 6, pp. 1863–1866, 1999. DOI: 10.1190/1.1444692.
[51] O. Anderson, "The Grüneisen ratio for the last 30 years," *Geophys. J. Int.*, vol. 143, no. 2, pp. 279–294, 2000. DOI: 10.1046/j.1365-246X.2000.01266.x.
[52] H. E. Jackson, C. T. Walker, and T. F. McNelly, "Second sound in NaF," *Phys. Rev. Lett.*, vol. 25, no. 1, pp. 26–28, 1970. DOI: 10.1103/PhysRevLett.25.26.
[53] J. M. Carcione, F. Cavallini, J. Ba, W. Cheng, and A. Qadrouh, "On the Kramers-Kronig relations," *Rheol. Acta*, vol. 58, no. 1–2, pp. 21–28, 2018a. DOI: 10.1007/s00397-018-1119-3.